Solid-liquid phase equilibria from free-energy perturbation calculations

Stefano Angioletti-Uberti,[1,*] Mark Asta,[2] Mike W. Finnis,[1] and P. D. Lee[1]
[1]*Department of Materials, Imperial College London, Prince Consort Road 20, SW72BP London, UK*
[2]*Department of Chemical Engineering and Materials Science, University of California–Davis, One Shields Ave., Davis, California, 95616-5294 USA*
(Received 6 August 2008; published 10 October 2008)

A method for calculating free-energy differences based on a free-energy perturbation (FEP) formalism in an alloy system described by two different Hamiltonians is reported. The intended application is the calculation of solid-liquid phase equilibria in alloys with the accuracy of first-principles electronic density-functional theory (DFT). For this purpose free energies are derived with a classical interatomic potential, and FEP calculations are used to compute corrections to these reference values. For practical applications of this approach, due to the relatively high computational cost of DFT calculations, it is critical that the FEP calculations converge rapidly in terms of the number of samples used to estimate relevant ensemble averages. This issue is investigated in the current study employing two classical interatomic-potential models for Ni-Cu. These models yield differences in predicted phase-boundary temperatures of approximately 100 K, comparable to those that might be expected between a DFT Hamiltonian and a well-fit classical potential. We show that for pure elements the FEP calculations converge rapidly with the number of samples, yielding free-energy differences converged to within a fraction of a meV/atom in a few dozen energy calculations. For a concentrated equiatomic alloy similar precision requires roughly a hundred samples. The results suggest that the proposed methodology could provide a computationally tractable framework for calculating solid-liquid phase equilibria in concentrated alloys with DFT accuracy.

DOI: 10.1103/PhysRevB.78.134203 PACS number(s): 64.10.+h, 31.15.xv

I. INTRODUCTION

Over the past two decades first-principles-based methods have been extensively developed for the calculation of solid-state alloy phase diagrams within the predictive framework of electronic density-functional theory (DFT).[1–7] These methods generally rely on the use of lattice-model Hamiltonians, with interaction parameters derived from first-principles calculations, to model the configurational energetics of solid alloy phases. The resulting model for alloy energetics is then combined with (quasi-) Harmonic theory and Monte Carlo simulations as a framework for computing vibrational and configurational contributions to finite-temperature free energies, respectively. The computational efficiency and predictive capabilities of such approaches have led to growing applications for metallic, semiconductor, and oxide systems. In contrast to this favorable situation for calculations of solid-state thermodynamic properties and phase boundaries, far less progress has been demonstrated to date in the application of first-principles methods for computing solid-liquid alloy phase equilibria.

While accurate *ab initio* calculations of melting lines have been demonstrated for pure elements and stoichiometric compounds based on quantum-molecular-dynamics (QMD) simulations,[8–11] these calculations are typically based on thermodynamic-integration techniques,[12] which are not easily generalized for applications to concentrated alloys with compositional disorder. To date first-principles calculations of alloy solid-liquid phase boundaries have been demonstrated from QMD thermodynamic-integration methods only in the limit of dilute solute compositions.[13,14] For concentrated alloys, the challenge lies in the need to average over the ionic configurational degrees of freedom, which for a solid substitutional alloy requires the use of Monte Carlo sampling methodologies, owing to the slow diffusive time scales over which these degrees of freedom are sampled in molecular dynamics (MD). For liquid-phase alloys, where diffusive time scales are much faster, sampling over the configurational degrees of freedom is possible by MD, but time scales on the order of tens of picoseconds are required, which are still relatively long for QMD simulations considering that several such runs at different compositions and temperatures are generally required to construct free-energy curves and associated phase boundaries.

In this paper we propose a framework that we expect to be useful for first-principles phase-boundary calculations in concentrated alloys based on the framework of thermodynamic free-energy perturbation (FEP) theory.[12,15] The basic approach is illustrated in Fig. 1. It involves the sampling of configurational and atomic displacement degrees of freedom employing a classical interatomic potential in Monte Carlo simulations to generate reference free-energy curves for solid and liquid phases, as illustrated by the dashed lines and open symbols in Fig. 1. Such calculations are further used to generate trajectories as the basis for FEP calculations and to compute the free-energy differences between the classical and DFT Hamiltonians, thus "correcting" the predictions of the classical potential, as illustrated by the solid lines and filled symbols in Fig. 1. The result of the procedure is then DFT-based results for solid and liquid free energies, which can be used both to construct phase boundaries, and to provide thermodynamic driving forces for continuum models for solidification kinetics.

The purpose of this work is to employ classical potentials to test the computational efficiency of the approach outlined above. The remainder of this paper is organized as follows. In Sec. II we review (i) a methodology for deriving the ref-

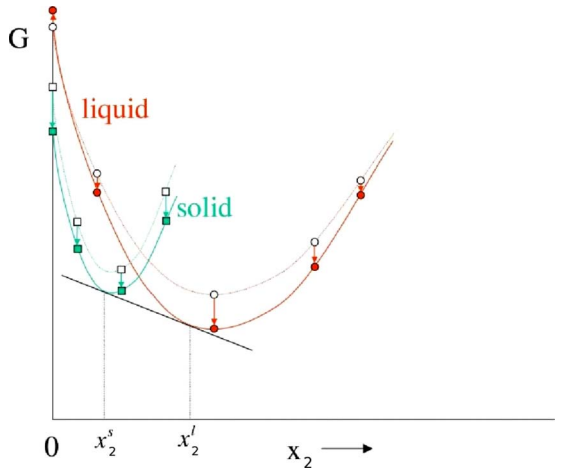

FIG. 1. (Color online) Schematic illustration of a two-step approach to calculate solid-liquid boundaries in concentrated alloys with *ab initio* accuracy. In the first step, the free energy versus concentration (mole fraction of element 2, x_2) curve is calculated using standard thermodynamic-integration techniques with a reference classical interatomic potential (open symbols) and fitting the calculated excess free energies to a polynomial expansion (see detail in the text). In the second step, a thermodynamic perturbation scheme is applied to calculate the difference in the free energy between the reference potential and a fully *ab initio* DFT calculation at several concentrations (filled symbols). The points so calculated can be used to refit the polynomial expansion of the excess free energy, thus gaining an *ab initio* accuracy in the calculations of concentrated-alloy free energies and associated solid and liquid phase-boundary compositions, x_2^s and x_2^l, respectively.

erence solid and liquid free-energy curves based on classical thermodynamic integration using semi-grand-canonical Monte Carlo methods and (ii) a free-energy perturbation approach for computing corrections to the resulting free-energy curves. The central issue concerning the practical implementation of this approach is the convergence of the second step with respect to number of samples employed in the estimation of relevant ensemble averages. We therefore present in Sec. III the results of a test based on the use of two different classical potentials that are known to give substantially different solid-liquid phase diagrams for the same system. The results of these tests suggest rapid convergence both for pure elements and for concentrated alloys. The results are discussed in Sec. IV and the main conclusions summarized in Sec. V.

II. METHODS

A. Thermodynamic-integration calculations of reference free energies

As described in Sec. I, the first step in the proposed approach involves the calculation of free energies as a function of composition for both solid and liquid alloy phases at fixed temperature and pressure. We briefly review here an approach that has been described in detail in previous publications.[16,17] The approach starts from the knowledge of the equilibrium melting temperature (T_{melting}) for the pure solvent material (referred to here as species 1), where the solid and liquid free energies are equal. The free-energy difference ($\Delta G_{\text{melting}}$) between solid and liquid phases at some particular temperature (T) above or below T_{melting} is determined by performing thermodynamic integration based on the Gibbs-Helmholtz relation:

$$\partial(\Delta G_{\text{melting}}/T)/\partial T = -\Delta H_{\text{melting}}/T^2, \tag{1}$$

where $\Delta G_{\text{melting}} = G_0^l - G_0^s$, G_0^α denotes the Gibbs free energy of phase α (solid or liquid) for pure species 1, and similarly for the enthalpy of melting, $\Delta H_{\text{melting}} = H_0^l - H_0^s$. The alloy free energy (G^α) as a function of composition is then computed by integrating the following relation:

$$\partial G^\alpha/\partial x_2 = \Delta\mu^\alpha, \tag{2}$$

where $\Delta\mu = \mu_2 - \mu_1$ is the difference in chemical potential between the solute and solvent species, and x_2 denotes the mole fraction of solute. This latter integration requires knowledge of the relationship $\Delta\mu(x_2)$ at constant temperature and pressure, which can be readily derived from Monte Carlo simulations employing a semi-grand-canonical (SGC) ensemble.[18]

For the purpose of performing the integration of Eq. (2), it is useful to fit an analytical form for $\Delta\mu$ by decomposing this quantity into ideal and excess contributions as follows:

$$\Delta\mu^\alpha(x_2) = k_B T \ln\frac{x_2}{1-x_2} + \Delta\mu_{xs}^\alpha(x_2), \tag{3}$$

where the last term ($\Delta\mu_{xs}^\alpha$) typically can be fit by a low-order polynomial for the purpose of integration. The result is an expression for the free energy of phase α that can be written in the following form:

$$G^\alpha(x_B,P,T) = G_0^\alpha(P,T) + k_B T[x_2 \ln(x_2) + (1-x_2)\ln(1-x_2)] + \sum_i^n A_i^\alpha(P,T)x_2^i, \tag{4}$$

where $G_0^\alpha(P,T)$ denotes the free energy of pure species 1 in the α phase, which needs only to be defined to within an arbitrary constant; this value can be assigned zero for one of the phases (e.g., solid) with the value for the other phase (e.g., liquid) being given by the free-energy difference ($\Delta G_{\text{melting}}$) as derived from the integration of Eq. (1). The polynomial coefficients (A_i^α) in Eq. (4) are obtained from the results of SGC Monte Carlo derived relationship between $\Delta\mu$ and x_2. Examples demonstrating the use of the approach described above are given in Refs. 16, 17, and 19.

B. Free-energy perturbation method

The procedure described in Sec. II A can be implemented straightforwardly with a classical interatomic-potential model to derive a reference free-energy curve. We turn next to the problem of correcting these reference free energies employing an approach that we will refer to as free energy peturbation (FEP) calculations. From Sec. II A, the free-energy curves for solid and liquid phases can be constructed from the knowledge of $\Delta G_0 = G_0^l - G_0^s$ (i.e., the difference in

free energies between liquid and solid phases for pure species 1), as well as the values of the polynomial coefficients A_i^α in each phase. The correction to the first term (ΔG_0) can be derived by computing the differences in elemental solid and liquid free energies between the reference and final Hamiltonians; similar calculations for alloys with a few different compositions can then be used to reoptimize the coefficients A_i in Eq. (4) to construct the final free-energy curve. In this paper we propose to calculate these free-energy corrections employing a FEP methodology, which dates back to Zwanzig.[15]

We concentrate here on the calculation of free-energy differences at zero pressure, where the Gibbs (G) and Helmholtz (F) free energies are equal, i.e., $G=F+PV=F$. Extension to finite pressure is straightforward. The *difference* in free energies between two systems A and B, whose thermodynamic properties are governed by the Hamiltonians H_A and H_B, can be written as

$$\beta\Delta F_{A\to B} = -\ln(\langle \exp -\beta(U_{A\to B})\rangle), \tag{5}$$

where $\beta=1/k_BT$ (k_B being Boltzmann's constant) and $U_{A\to B}$ is the potential energy difference calculated for the same configuration using the two different Hamiltonians H_A and H_B. The brackets $\langle\cdots\rangle$ indicate a canonical ensemble average over the configurations of system A only. It is interesting to note that this FEP formula can be thought of as a particular case of Jarzynski's relation[20] connecting nonequilibrium work values and free-energy differences:

$$\beta\Delta F_{A\to B} = -\ln(\langle \exp(-\beta W_{A\to B})\rangle), \tag{6}$$

where $W_{A\to B}$ is now the work done along any path connecting A to B. The FEP procedure can be thought of as a limit of Eq. (6), where one takes a nonequilibrium path involving an infinitely quick switch between the two states.

In practical applications, the ensemble average in Eq. (5) is approximated by a finite sum over N configurations (σ) generated from an equilibrium NVT (constant number of particles N, volume V and temperture T) molecular dynamics or Monte Carlo simulation for system A:

$$\beta\Delta F_{A\to B} = -\ln\left[\frac{1}{N}\sum_{\sigma=1}^{N}\exp[-\beta U_{A\to B}(\sigma)]\right]. \tag{7}$$

Compared to commonly used equilibrium thermodynamic-integration approaches, this FEP formulation is conceptually simpler as no information other than the internal energy of the system is needed and the approach avoids the necessity of equilibrating the final state configurations, which would otherwise give an added computational cost. However, the use of FEP formalism for the calculations of free-energy differences has been shown in many cases to suffer from convergence problems and associated overbias of free-energy differences. Several studies have been undertaken to understand the origins of these problems (see Refs. 21–25), and it has been shown that they arise from the entropy difference between the target and reference system. As will be discussed below, rapid convergence of Eq. (7) requires that systems A and B are sufficiently "close" in the sense that will be described in Sec. IV. Hence, the purpose of the calculations described in Secs. III and IV is to assess the convergence properties of Eq. (7) for two classical interatomic-potential systems giving differences in energy and phase diagrams comparable to those expected between a good classical interatomic potential and a DFT Hamiltonian.

C. Implementation

As described in Sec. II B, rapid convergence of Eq. (7) can be expected if the configurational energetics of the reference Hamiltonian are sufficiently close to those of the final state. Efficient applications of the FEP formalism involving the use of DFT Hamiltonians as the target result thus require high-quality classical potentials, which in practice may be obtained by fitting to an extensive enough set of data generated from the DFT Hamiltonian.

To better quantify the statistical convergence properties of Eq. (7) we consider here a test system, namely, Ni-Cu. We do not undertake DFT calculations in this analysis but rather choose as the reference and target systems (i.e., systems A and B in the notation of the previous section) two classical Hamiltonians that are known to give rise to significantly different phase boundaries (e.g., solidus and liquidus boundaries differing by roughly 100 K) for this system.

We choose as our reference and target systems the embedded-atom-method (EAM) Cu-Ni potentials due to Foiles[26] (referred to hereafter as the "smf7" potential) and Foiles, Baskes, and Daw[27] (referred to hereafter as the "$u3$" potential), respectively. From coexistence simulations the melting temperatures of the smf7 and $u3$ potentials for elemental Ni have previously been calculated to be approximately 1820 and 1710 K, respectively.[28,29] For use in Sec. III, we will take the difference in melting temperature between the target ($u3$) and reference (smf7) systems as $\Delta T_{\text{melting}}=-110$ K with an estimated standard statistical uncertainty of 5 K.

To apply the FEP method to compute the free-energy differences between reference and target potentials for pure elements, the configurations σ in Eq. (7) were generated employing standard NVT molecular-dynamics simulations with a system size of 500 atoms (corresponding to $5\times5\times5$ fcc unit cells for the solid phase) and periodic boundary conditions (subsequent NPT (constant number of particles N, pressure P and temperature T) dynamics simulations were also performed to compute pressure corrections to melting temperatures as described in Appendix). Temperature was maintained constant using a Nose-Hoover thermostat (similarly, pressure in the NPT simulations was maintained with a Nose-Hoover barostat)[30] and the integration of the equations of motion was performed using a velocity-Verlet algorithm[12] with a time step of 2 ps. All simulations were based on the use of the LAMMPS code.[31] Simulations were performed at a temperature of 1820 K for pure Ni. The MD trajectories were used to generate statistically independent states collecting one configuration every 0.1 ps. Through these configurations the free-energy difference is calculated through Eq. (7) by computing $U_{A\to B}$ as the difference in potential energies between the reference and target potential for each sampled configuration.

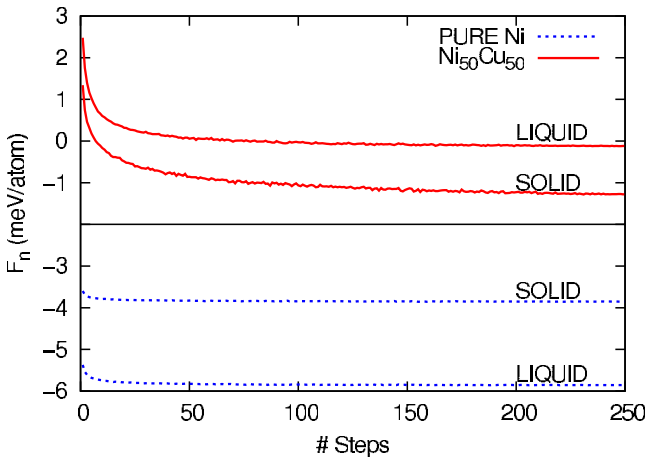

FIG. 2. (Color online) Free-energy difference as given in Eq. (17) as a function of the number of steps (N) taken into consideration in the averaging. The bottom panel presents free-energy differences between the $u3$ and smf7 potentials for solid and liquid phases of elemental Ni. The top panel represents free-energy differences between solid-solution and liquid phases of a concentrated $Ni_{50}Cu_{50}$ alloy.

In addition to considering pure elements, we applied the FEP method to compute free-energy differences between reference and target potentials for a concentrated equiatomic ($x_{Ni}=0.5$) alloy using Monte Carlo simulations in a canonical (NVT) ensemble with the volume V chosen to give zero pressure for the reference system. As in the MD simulations, we employed 500-atom supercells with periodic boundary conditions. The displacement and configurational degrees of freedom of the alloy were sampled through Monte Carlo steps that involved selecting two atoms at random and attempting displacements of each with a maximum value of 0.2 Å along each Cartesian direction, coupled with an attempted exchange of species if the two atoms selected were of opposite type. These attempted moves were accepted or rejected based on the Metropolis algorithm appropriate for a canonical ensemble at a temperature of 1500 K. A total of 500 independent configurations were generated from these simulations for use in Eq. (7).

III. RESULTS

Figure 2 plots the value of the calculated free-energy differences between target and reference systems as a function of the number of steps (N) taken into consideration in Eq. (7) for both the solid and liquid phases in the pure system (bottom panel) and in the concentrated $Ni_{50}Cu_{50}$ alloy (top panel). We report the results in the form of block averages as defined in Ref. 32.

The results in Fig. 2 show that the calculated free-energy values converge very rapidly for the pure element, for both the liquid and solid phases, with only a few times ten steps required to obtain results converged to within a fraction of a meV per atom. For the alloy the convergence is clearly seen to be slower (especially in the solid phase); however, convergence to a fraction of a meV/atom is still achievable in approximately 100 steps, a value of N which is definitely achievable in an *ab initio* DFT framework. Moreover, a correction to the results to estimate the $N\rightarrow\infty$ limit could be applied if needed, further improving the accuracy of the result. As shown in Refs. 21, 22, and 32, this correction generally implies writing the free-energy variation as block averages (defined in the references above) and fitting it to a polynomial of the form

$$\Delta F_N = \Delta F_\infty + \phi_1 (1/N)_1^\tau, \tag{8}$$

where τ_1 and ϕ_1 are fitting parameters and N is the number of work values included in the definition of the block average. A theoretical justification for this form of the fitting function is given in Ref. 21, while for practical applications the reader is referred to Refs. 22 and 32.

To check that the results in Fig. 2 are converging to the correct values, we use these numbers to perform a calculation of the difference in melting points predicted by the two Ni potentials for comparison with the value of $\Delta T_{\text{melting}} = -110 \pm 25$ K derived from coexistence simulations. For this purpose we make use of the following relationship between $\Delta G_{\text{melting}} = G^l - G^s$ and temperature:

$$\frac{\Delta G_{\text{melting}}}{L_{\text{melting}}} = 1 - \frac{T}{T_{\text{melting}}}, \tag{9}$$

where L_{melting} is the enthalpy of melting (i.e., the latent heat of fusion at constant pressure). Equation (9) can be derived from the classical Vant'Hoff equation[33] under the assumption that L does not vary in the interval $[T\text{-}T_{\text{melt}}]$, which is a valid assumption in this case. For the reference smf7 potential we have performed simulations at the equilibrium melting temperature, $T^{\text{smf7}}_{\text{melting}} = 1820$ K, where $\Delta G^{\text{smf7}}_{\text{melting}} = 0$. The melting temperature for the target $u3$ potential (T^{u3}_{melting}) can then be derived with the aid of Eq. (9) using the calculated value of $\Delta G^{u3}_{\text{melting}}$ obtained from the solid and liquid free energies in Fig. 2 as follows:

$$\frac{T^{\text{smf7}}_{\text{melting}}}{T^{u3}_{\text{melting}}} = 1 - \frac{\Delta G^{u3}_{\text{melting}}}{L^{u3}_{\text{melting}}}. \tag{10}$$

As we are interested in the zero-pressure melting point, we have $G=F$. Calculation of $\Delta F_{\text{melting}}$ is performed by application of Eq. (7). We refer to the Appendix for further details of this calculation.

In Fig. 3 we present the calculated difference in melting temperatures as a function of the number of samples (N) used in the FEP formula Eq. (7). The present results lead to a predicted melting temperature of approximately 1711.5 K, which agrees with the value of 1710 K derived from previous coexistence simulations, within the statistical uncertainty of 5 K quoted above. We also note that the present results for $\Delta T_{\text{melting}}$ are seen to converge to within a fraction of a Kelvin within a few dozen samples. The results thus suggest that the formalism outlined in this paper may provide an extremely efficient method for obtaining melting points of metals from DFT calculations, employing FEP calculations based on reference classical EAM potentials.

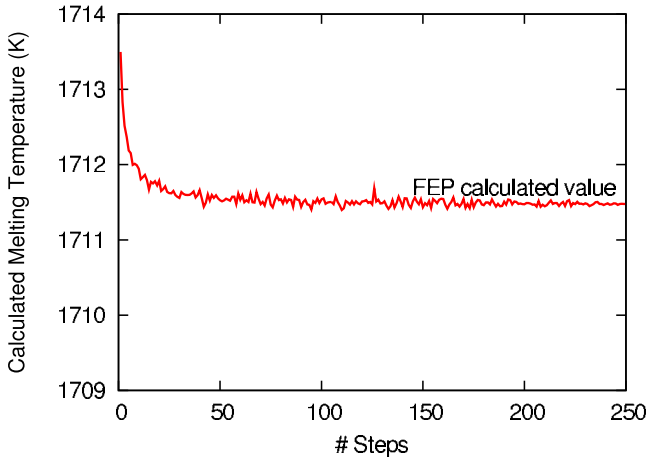

FIG. 3. (Color online) Calculated difference in melting temperatures for Ni from smf7 and $u3$ potentials, as a function of the number of steps taken in consideration in the FEP average (red curve).

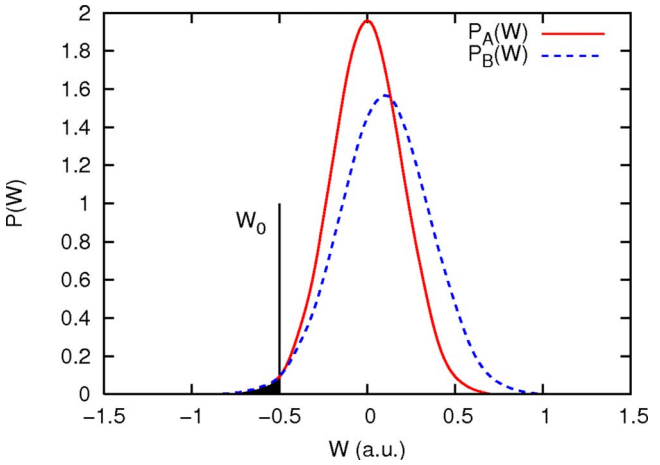

FIG. 4. (Color online) Graphical representation of Eq. (11). The fractional inaccuracy for a given simulation attempting to calculate a free-energy difference between system A and B is given by the area under P_B below a certain value W_0. Above W_0 complete sampling of P_A is assumed (Ref. 23). Gaussian distributions are shown for illustrative purposes, although the real distributions need not be Gaussian in an actual simulation.

IV. DISCUSSION

We turn now to a discussion of the factors underlying the relatively fast convergence of Eq. (7) in our calculations, and the implications of our results for free-energy calculations in alloys. The formal mathematical model on which our argument is based was first developed by Lu and Kofke in Ref. 23, where they have shown that, under some basic assumptions, the exponential fractional inaccuracy of the calculated free-energy difference (i.e., the difference between the exponential of the true and calculated free-energy difference with respect to the former) can be written as

$$\frac{\exp(-\beta\Delta F_{\text{true}}) - \exp(-\beta\Delta F_{\text{calc},A})}{\exp(-\beta\Delta F_{\text{true}})} = \int_{-\infty}^{W_0} P_B(W)dW, \tag{11}$$

where the subscripts A and B refer to the choice of the particular reference system, $P_X(W)$ is the distribution of the work values (i.e., the difference in energy in our case) obtained in going from the reference (X) to the target system, and W_0 is the work value above which complete sampling is assumed. A graphical interpretation of Eq. (11) shows that the inaccuracy in the estimate $(\Delta F_{\text{calc},A})$ of the free energy calculated going from A to B is given by the area under the probability distribution $P_B(W)$ of work values one would obtain going from B to A (i.e., taking B as the reference system), see for reference Fig. 4.

The most important message that one can obtain from Eq. (11) is that the FEP formula can be successfully used only in those cases where the two systems under consideration generate highly overlapping work distributions. This condition is obtained if, as in our case, the Hamiltonians describing the two systems A and B mainly sample the same part of the phase space. To clarify this point consider the following qualitative model (see Fig. 5 for reference), which we hope can give some more insights on the physics underlying the problem.

Suppose that a particular configuration Γ has a high probability of appearing in system A because it is a low-energy configuration but has a low probability of being observed in system B, where it has a high energy (left image in Fig. 5). For this configuration swapping between the two different potentials gives rise to a work value of $\bar{W}=U_B-U_A$. Finding a value $\bar{W}$ starting from system A has a high probability, i.e., $P_A(\bar{W})$ is high. However, as Γ is a high-energy configuration in the B system this will rarely be sampled starting from system B so $P_B(\bar{W})$ is low, and thus the overlap between the two work distribution curves and hence the accuracy of the calculations will be low. The same explanation can be used where the configuration Γ is now a low-energy configuration for both potentials; in this case though one will have a very good overlap between $P_A(\bar{W})$ and $P_B(\bar{W})$ and a high accuracy will be obtained (right image in Fig. 5). In the present work the rapid convergence to the correct value of the free-energy difference calculations implies that the two different EAM potentials for Ni-Cu are apparently close enough to sample similar regions of phase space.

We believe our result to be quite general and that a similarly rapid convergence can be obtained for other systems as well. Since the pioneering work of Ercolessi and Adams[34] in the early 90's, the development of interatomic potentials based on fitting to *ab initio* results has become relatively standard practice. This approach has been used for a variety of systems including pure metals,[35,36] alloys,[37–39] and other inorganic compounds.[40,41] As these potentials are constructed to accurately reproduce *ab initio* energies for many different configurations, they are natural candidates for applications of the method we have described. Moreover, if the spread in the energies is still too high to achieve rapid convergence, the newly calculated *ab initio* energies can be included in the database to refit the potential, improving its accuracy and thus enhancing convergence with little additional computational cost.

The results of this work suggest that it should be feasible

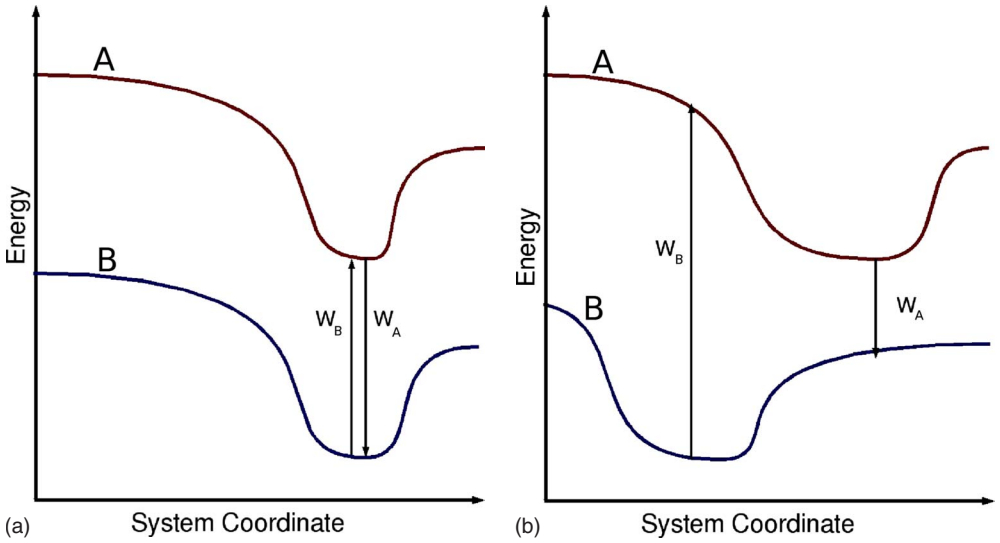

FIG. 5. (Color online) Comparison of work values W given by direct ($A \rightarrow B$) and inverse ($B \rightarrow A$) processes and their relationship to the energy landscape (here exemplified as a single coordinate system). The arrows indicate the most probable work value sampled W_X starting from system x. (a) The probability of direct and reverse observation of a work value W is high in both systems; hence, convergence is fast. (b) Configurations sampled by system A and system B are rarely the same, the generated work distribution will poorly overlap leading to slow convergence.

to use the FEP approach for a target system involving an *ab initio* potential, as a framework for calculating accurate *ab initio* free-energy differences in a straightforward and computationally tractable manner, even for concentrated alloys where alternative approaches involving equilibrium thermodynamic-integration methods are expected to be much more computationally expensive. We want to stress here that the availability of a good, starting potential (i.e., one close to the target Hamiltonian) is an absolutely necessary prerequisite for such applications involving DFT target Hamiltonians. A potential which leads to energy difference significantly different from DFT would give rise to a slower convergence rate of Eq. (7).

Our approach is related to that recently proposed by Greeff in Ref. 42. In that paper only the case of a pure liquid is considered and the free-energy difference is calculated by a truncated cumulant expansion of Eq. (5). We have shown here our nonperturbative method is viable for a concentrated alloy in both solid and liquid phases. The perturbative approach of Greeff should also be applicable to alloys, but the trade off between computational time and accuracy has not yet been studied.

V. CONCLUSIONS

In this paper, we have demonstrated that it is possible to calculate free-energy differences in both elemental metals and concentrated alloys in an accurate and computationally efficient manner within a simple FEP formalism. We demonstrate that for typical differences one would expect between two reasonably accurate potential energy descriptions in a metal, free-energy values can be calculated to a precision better than 1 meV/atom within approximately a hundred sampling steps. We further establish that the values obtained from the FEP formalism converge to the correct limits by using the calculated free energies to compute the melting temperature of Ni using a EAM potential for which the presents results are within the statistical error bars of the values derived independently from coexistence simulations.[28,29]

The present calculations are found to suffer only weakly from the convergence problems that can be present in using a FEP formalism. We discuss how this finding can be associated with the relatively small differences in entropy between the reference and target systems, meaning that the systems can be considered to be small perturbations from one another. We expect that the approach outlined in this paper offers a reasonably efficient way to tackle the problem of calculating solid-liquid phase boundaries in alloys with DFT accuracy over the entire composition range.

ACKNOWLEDGMENTS

We acknowledge Paul Tangney and Adrian Sutton for useful discussions on the general ideas behind the paper, Dario Alfe' and Mike Gillan for pointing out to us some issues relating the choice of reference system to the rate of convergence, and Dann Frenkel for his lectures given during the CECAM tutorial (Amsterdam), which helped inspire this work. We also want to acknowledge EPSRC under Grant No. EP/D04619X and the Royal Academy of Engineering for funding. M.A. acknowledges support from the U.S. Department of Energy, Office of Basic Energy Sciences, under Contract No. DE-FG-02-06ER46282.

APPENDIX

Calculation of $\Delta F_{\text{melting}}$ in our framework needs in principle the calculation of two different terms for both the solid and liquid phase, provided the simulation temperature is the same:

$$F_\alpha^A(V_\alpha^A,T) = F_\alpha^B(V_\alpha^B,T) + \int_{V_\alpha^B}^{V_\alpha^A} \left.\frac{\partial F_\alpha^B(V,T)}{\partial V}\right|_T dV - \Delta F^{A\to B}, \tag{12}$$

$$\Delta F^{A\to B} = F_\alpha^B(V_\alpha^A,T) - F_\alpha^A(V_\alpha^A,T). \tag{13}$$

Here the superscript refers to the two different potentials between which the free-energy difference has to be calculated and the Greek subscript to the phase (here solid or liquid). Further, V_α^A is the equilibrium volume of phase α at the temperature for which sampling has been made for potential A (the smf7 potential in our case), i.e., what is referred to here as T^A. By contrast, V_α^B is the equilibrium volume of phase α at the melting temperature T^B calculated in some other simulation using potential B (the $u3$ potential in our case).

Using the thermodynamic identities

$$\left.\frac{\partial F_\alpha(V,T)}{\partial V}\right|_T = -p_\alpha, \tag{14}$$

combined with Eq. (12) yield

$$\Delta F_{\text{melting}}^A(V_{\alpha/\beta}^A,T) = F_{\text{melting}}^B(V_{\alpha/\beta}^B,T) - \int_{V_\beta^B}^{V_\beta^A} p_\beta^B dV + \int_{V_\alpha^B}^{V_\alpha^A} p_\alpha^A dV - \Delta F^{A\to B}(V_\alpha^A,T). \tag{15}$$

The first term on the right-hand side is zero since we start our simulation at the melting temperature of the reference potential (smf7) and is thus the free energy of melting is by definition zero. The second and third terms are pressure terms, which depend on the fact that the equilibrium volumes are not necessarily the same for the two different potentials.

For what concerns the pressure term in Eq. (15), $p_{\alpha,\beta}^B(V_{\alpha,\beta}^B,T)=0$, and we take in the integration $p_{\alpha,\beta}^B=\text{const}=p_{\alpha,\beta}^B(V_{\alpha,\beta}^A,T)/2$, i.e., we considered p linearly increasing in the interval $[V^B-V^A]$. This assumption is found to be well justified from the behavior of the computed pressure during the simulation.

Under the above assumptions, Eq. (15) can be rewritten as follows:

$$\Delta F_{\text{melting}}^A(V_{\alpha/\beta}^B,T) = -\frac{1}{2}p_\beta^B(V_\beta^A,T)[V_\beta^A(T) - V_\beta^B(T)] + \frac{1}{2}p_\alpha^B(V_\alpha^A,T)[V_\alpha^A(T) - V_\alpha^B(T)] - \Delta F_{\text{melting}}^{A\to B}(V_\alpha^A,T). \tag{16}$$

Considering the last term in Eq. (16) by applying the FEP equation, we have for both solid and liquid

$$\Delta F_{A\to B} = -\frac{1}{\beta}\langle \exp -\beta(U_B - U_A)\rangle_A. \tag{17}$$

This average is calculated by taking snapshots of the configurations generated through MD with the smf7 potential every 100 fs in order to avoid statistical correlations between them, switching to the u3 potential and calculating U_A-U_B.

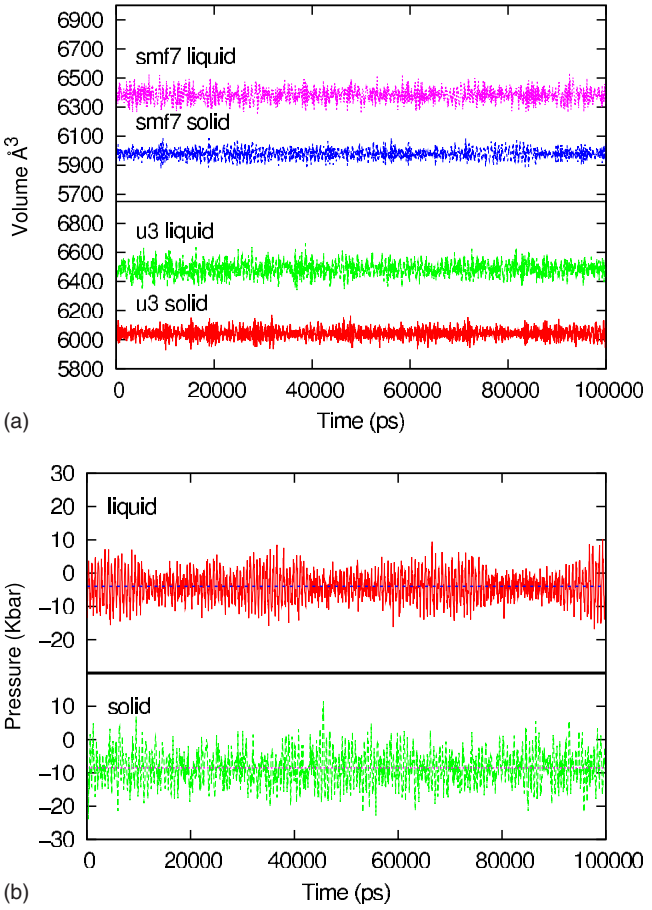

FIG. 6. (Color online) (a) Fluctuation of volume during NPT simulations at 0 pressure for $u3$ and smf7 potentials. Notice that the difference in the equilibrium volume given by the two potentials is close to zero. (b) NVT simulation using the smf7 potential at $V=V^{u3}$ to calculate the average pressure during the run. As there is little difference in the calculated equilibrium volumes, the average pressure is almost zero, hence, the little correction in Eq. (15) due to the pressure term.

Figure 6 shows the results of NPT MD simulations to determine the equilibrium volumes of both the $u3$ and smf7 potentials.

From these simulations we calculated the pressure term, which is here equal to

$$\begin{aligned}\Delta F^{\text{pressure}} &= -\frac{1}{2}p_\beta^{\text{smf7}}(V_\beta^{u3},T)[V_\beta^{u3}(T) - V_\beta^{\text{smf7}}(T)] \\ &\quad + \frac{1}{2}p_\alpha^{\text{smf7}}(V_\alpha^{u3},T)[V_\alpha^{u3}(T) - V_\alpha^{\text{smf7}}(T)] \\ &= -\frac{1}{2}(-8.519\ \text{Kbar})(6455\ \text{Å}^3 - 6381\ \text{Å}^3) \\ &\quad + \frac{1}{2}(-3.947\ \text{Kbar})(6001\ \text{Å}^3 - 5978\ \text{Å}^3) \\ &= 169\ \text{meV} = 0.34\ \text{meV/atom}.\end{aligned}$$

This value is definitely negligible.

*sangiole@imperial.ac.uk

[1] A. F. Kohan, P. D. Tepesch, G. Ceder, and C. Wolverton, Comput. Mater. Sci. **9**, 389 (1998).
[2] A. Van de Walle, G. Ghosh, and M. Asta, in *Applied Computational Materials Modeling: Theory, Simulation and Experiment*, edited by G. Bozzolo, R. D. Noebe, and P. Abel (Springer, New York, 2007).
[3] M. Asta, V. Ozolins, and C. Woodward, JOM **53**, 16 (2001).
[4] G. Ceder, A. Van der Ven, C. Marianetti, and D. Morgan, Modell. Simul. Mater. Sci. Eng. **8**, 311 (2000).
[5] F. Ducastelle, *Order and Phase Stability in Alloys*, 1st ed. (Elsevier Science, New York, 1991).
[6] A. van de Walle and M. Asta, in *Handbook of Materials Modeling*, edited by S. Yip (Springer, New York, 2005).
[7] A. Zunger, in *Nato Advanced Study Institute on Statistics and Dynamics of Alloy Phase Transformations*, edited by P. Press (Plenum, New York, 1994).
[8] G. A. de Wijs, G. Kresse, and M. J. Gillan, Phys. Rev. B **57**, 8223 (1998).
[9] D. Alfè, G. D. Price, and M. J. Gillan, Phys. Rev. B **65**, 165118 (2002).
[10] D. Alfè, Phys. Rev. Lett. **94**, 235701 (2005).
[11] O. Sugino and R. Car, Phys. Rev. Lett. **74**, 1823 (1995).
[12] D. Frenkel and B. Smith, *Understanding Molecular Simulations*, Computational Science Vol. 1, 2nd ed. (Academic, San Diego, 1996).
[13] D. Alfè, G. A. De Wijs, G. Kresse, and M. J. Gillan, Int. J. Quantum Chem. **77**, 871 (2000).
[14] D. Alfè, M. J. Gillan, and G. D. Price, J. Chem. Phys. **116**, 7127 (2002).
[15] R. Zwanzig, J. Chem. Phys. **22**, 1420 (1954).
[16] C. Becker, M. Asta, J. Hoyt, and S. Foiles, J. Chem. Phys. **124**, 164708 (2006).
[17] J. Hoyt, J. W. Garvin, E. Webb, and M. Asta, Modell. Simul. Mater. Sci. Eng. **11**, 287 (2003).
[18] D. A. Kofke and E. D. Glandt, J. Chem. Phys. **87**, 4881 (1987).
[19] M. Asta, D. Sun, and J. Hoyt, *Thermodynamics, Microstructure and Plasticity*, edited by A. Finel, D. Mazière, and M. Veron (Kluwer, Boston, 2003).
[20] C. Jarzynski, Phys. Rev. Lett. **78**, 2690 (1997).
[21] D. M. Zuckerman and T. B. Woolf, Phys. Rev. Lett. **89**, 180602 (2002).
[22] D. M. Zuckerman and T. B. Woolf, Chem. Phys. Lett. **351**, 445 (2002).
[23] N. D. Lu and D. A. Kofke, J. Chem. Phys. **114**, 7303 (2001).
[24] N. Lu, J. Adhikari, and D. A. Kofke, Phys. Rev. E **68**, 026122 (2003).
[25] N. D. Lu and D. A. Kofke, J. Chem. Phys. **115**, 6866 (2001).
[26] S. M. Foiles, Phys. Rev. B **32**, 7685 (1985).
[27] M. S. Daw, S. M. Foiles, and M. I. Baskes, Mater. Sci. Rep. **9**, 251 (1993).
[28] D. Sun, M. Asta, and J. Hoyt, Phys. Rev. B **69**, 024108 (2004).
[29] M. Asta, J. Hoyt, and A. Karma, Phys. Rev. B **66**, 100101 (2002).
[30] S. Nose, J. Chem. Phys. **81**, 511 (1984).
[31] S. J. Plimpton, J. Comput. Phys. **117**, 1 (1995).
[32] F. M. Ytreberg and D. M. Zuckerman, J. Comput. Chem. **25**, 1749 (2004).
[33] P. Atkins and J. De Paula, *Physical Chemistry*, 8th ed. (Oxford University Press, Oxford, 2007).
[34] F. Ercolessi and J. B. Adams, Europhys. Lett. **26**, 583 (1994).
[35] X. Y. Liu, J. B. Adams, F. Ercolessi, and J. A. Moriarty, Modell. Simul. Mater. Sci. Eng. **4**, 293 (1996).
[36] X. Y. Liu, F. Ercolessi, and J. B. Adams, Modell. Simul. Mater. Sci. Eng. **12**, 665 (2004).
[37] R. R. Zope and Y. Mishin, Phys. Rev. B **68**, 024102 (2003).
[38] P. Williams, Y. Mishin, and J. Hamilton, Modell. Simul. Mater. Sci. Eng. **14**, 817 (2006).
[39] Y. Mishin, Acta Mater. **52**, 1451 (2004).
[40] P. Tangney and S. Scandolo, J. Chem. Phys. **119**, 9673 (2003).
[41] P. Tangney and S. Scandolo, J. Chem. Phys. **117**, 8898 (2002).
[42] C. W. Greeff, J. Chem. Phys. **128**, 184104 (2008).